

Characteristic slip for five great earthquakes along the Fuyun fault in China

Y. Klinger¹*, M. Etchebes¹, P. Tapponnier² and C. Narteau¹

The seismic hazard associated with an individual fault can be assessed from the distributions of slip and recurrence times of earthquakes. However, seismic cycle models¹ that aim to predict rupture lengths and fault displacements of successive earthquakes on one fault remain poorly validated. It is therefore unknown whether individual fault segments rupture independently, producing earthquakes with a diverse range of magnitudes and recurrence times, or slip by characteristic amounts, with characteristic magnitudes. Here we use high-resolution satellite data to document the horizontal offsets of stream channels and terraces created by strike-slip motion on the Fuyun fault, Xinjiang, China, during five historical earthquakes. We find that the M_s 7.9 11 August 1931 earthquake produced a surface rupture with a length of 160 km, dispersed over three different fault segments. The 290 measured stream channel and terrace offsets record an average slip of 6.3 m. We use the degree of preservation of geomorphological markers to assign relative ages to individual fault offsets and identify at least four distinct older earthquakes. We find that these older earthquakes also produced fault offsets with a similar distribution to the 1931 earthquake. As the slip distributions during five successive earthquakes were so similar, we conclude that ruptures on the Fuyun fault obey a characteristic slip model.

Very few large earthquakes are known to have ruptured the same fault segment twice in historical or instrumental time¹. The formulation of slip- and time-predictable seismic cycle models is primarily based on the recurrence of moderate to small magnitude earthquakes^{2,3}. Palaeo-earthquake time series most often show two to four, but rarely ten or more events^{4–6}. Even rarer are palaeo-seismological sites where both horizontal coseismic displacements and dated event horizons are documented^{7–9}. Earthquakes with surface ruptures mapped to a level of detail sufficient to discuss the interplay between fault geometry and rupture processes are also few^{10,11}. Thus, earthquake rupture and recurrence models are constrained by very limited datasets. Field studies directed at testing such models must target sites where the known slip function of the last event can be used for calibration, and where clear evidence of past earthquake offsets are preserved. So far, only a handful such sites are documented, notably on the Superstition Hills fault¹² and along some sections of the North Anatolian fault¹³.

On 11 August, 1931, the Fuyun earthquake ruptured the right-lateral Fuyun fault (Fig. 1) in the southern Altai Mountains of Northwest China^{14,15}. With an estimated M_s of 7.9 (ref. 16), this event ranks among the largest continental strike-slip earthquakes of the past century. Surface breaks were mapped over ≈ 160 km, with average lateral slip in excess of several metres^{17,18}. As a result of the

rather arid climate and limited human degradation, such breaks are remarkably preserved today.

With specifically acquired panchromatic Quickbird satellite images (~ 60 cm pixels, geo-referenced) along a 5 km wide swath straddling the length of the fault (Fig. 1), we mapped the 1931 rupture in detail, except for its 40 km-long northern section, which was obscured by clouds. Three principal segments can be defined, based on steps or significant azimuth changes ($>5^\circ$). In addition to right-lateral slip, normal throw along the northern, Kokotohai segment has led to damming of the Irtysh and tributary rivers into permanent lakes. By contrast, thrust faulting is locally observed on the southern and central segments, particularly near Karaxingar.

Along 110 km (70%) of the rupture, geomorphic piercing lines defined by stream channels and terrace risers were systematically identified to measure coseismic horizontal offsets. The measurements were performed by best retrofitting the geomorphic markers into initial alignment (Fig. 2, Supplementary Method Section, Fig. S1a and Fig. S2a–n). This yielded a total of 569 horizontal offset measurements ranging between 2.2 ± 0.6 m and 64.5 ± 0.6 m (Fig. 1, Supplementary Table S1). The attached uncertainties include marker sharpness, rupture zone width and piercing line obliquity, besides the intrinsic error owing to image resolution (~ 60 cm). Overall, they are on the order of 10% for 208 measurements, between 10% and 20% for 273 measurements, and $>20\%$ for 88 measurements. The data are not distributed evenly along the rupture, the most active outwashes being unable to preserve offset markers except for short periods of time. An assessment of the robustness of each measurement is also proposed, based on along-strike offset consistency to distances of 100 m on either side (Supplementary Table S1). Reconstructing piercing line alignment typically meets with difficulties owing to marker erosion¹⁹, but calibration of key offsets in the field (Supplementary Fig. S1b) was used to alleviate such difficulties and further validate the Quickbird dataset.

Although coseismic slip variability over short distances is commonly observed^{20,21}, co-located twofold to threefold multiples imply that the Fuyun dataset includes 1931 coseismic offsets as well as cumulative offsets owing to older events. Hence, the dataset may be split into two subsets. The subset grouping the smallest offsets at each site (290 measurements) defines the coseismic slip during the 1931 earthquake. It is quite similar to that derived from smaller 1931 rupture datasets obtained in the field^{17,22} (Supplementary Fig. S3 and Table S2). Each subset is then analysed independently to characterize slip distributions.

The 290 offset measurements attributed to the 1931 rupture indicate an average coseismic slip l_c of $6.3 \text{ m} \pm 1.2$. The northern

¹Institut de Physique du Globe de Paris, Sorbonne Paris Cité, Univ. Paris Diderot, UMR 7154 CNRS, 1 rue Jussieu, F-75005 Paris, France, ²EOS, Nanyang Technological University, N2-01A-09, 50 Nanyang Avenue, Singapore 639798. *e-mail: klinger@ipgp.fr.

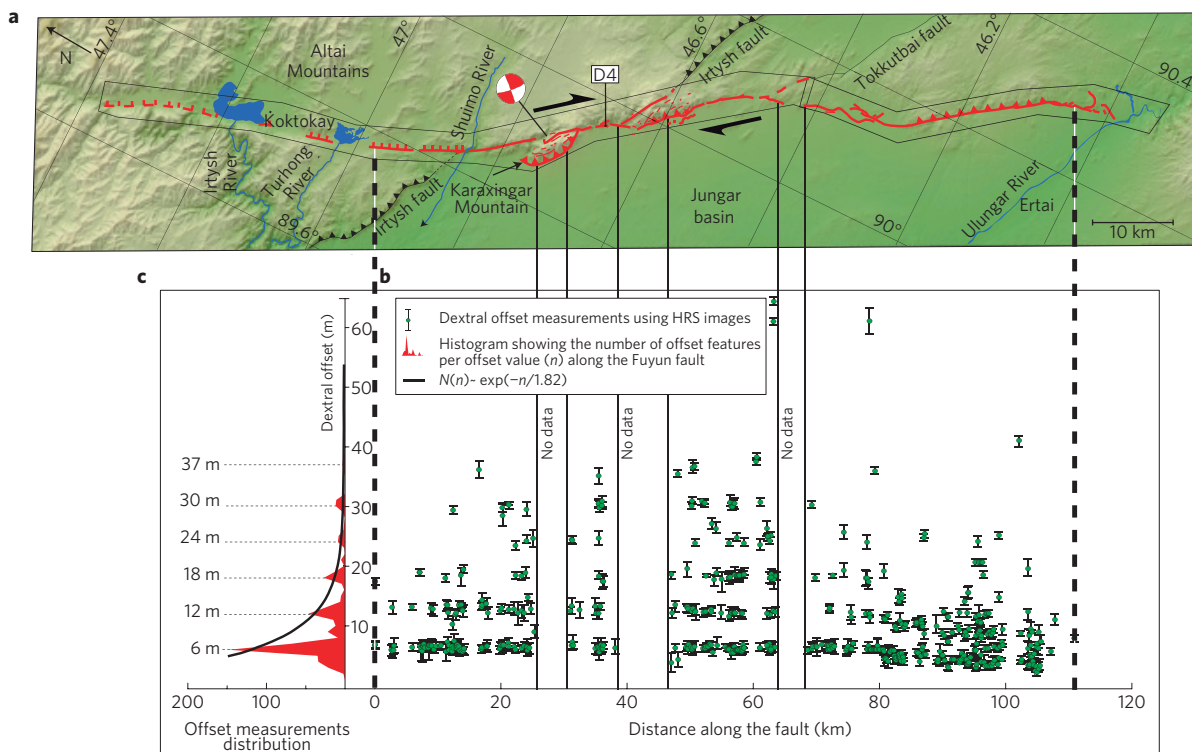


Figure 1 | Rupture map and offset measurements. **a**, 1931 rupture trace (red), mapped from Quickbird satellite image swath (swath limits indicated by thin lines). **b**, 569 horizontal offset measurements along the south-central part of the rupture from retrofitting of geomorphic markers into initial alignment. Error bars depend on the quality of measurements (see text and Supplementary Material for discussion). **c**, Horizontal offset distribution. Note the number of measurements decreasing exponentially with increasing offset size.

40 km of rupture, where normal faulting is dominant, is not included in this average. Based on this average value, scaling laws linking magnitude, average-slip and rupture-length for strike-slip earthquakes²³ yield $M_w = 7.6$, consistent with the magnitude M_s (7.9) derived from seismological data²⁴. The slip distribution obtained (Fig. 1) shows no prominent displacement peak, even though one might be possible in the field near Karaxingar²² (Supplementary Fig. S3 and Table S2). Sections with smaller than average coseismic slip, often marking segment boundaries^{21,25}, are not observed either. We cannot exclude the possibility that either minimum or maximum values might be located in some of the Quickbird data gaps, but outside such gaps the 1931 earthquake slip function does look unusually uniform, unlike those of several other earthquakes of similar magnitude, which show more variability along strike^{21,25–27}.

We interpret the second data subset of 279 larger offsets as representing the cumulative effect of several earthquakes, including the 1931 event. The implicit assumption—that the climatic modification of landforms occurs faster than earthquake disruption—seems justified by the slow slip-rate²⁸ and the millennial return time of great events²⁹ in a temperate continental climatic environment at latitude 46–47°N. The statistical distribution of cumulative offsets shows at least three well-defined and well-separated peaks, and more in places (Fig. 1). Such peaks are best documented along the northern and, most remarkably, central segment, where up to five regularly spaced clusters of values are clear. Using a discrete Fourier transform (Supplementary Method, Figs S4 and S5), we determine the characteristic wavelength Λ of the distribution to be 6.24 m, on par with the average slip l_c of the 1931 event. This indicates that, within error, the successive peaks at 12, 18, 24, 30 and possibly even 37 m in the offset distribution (Fig. 1) may represent the added displacements of 2, 3, 4, 5 and perhaps 6 great earthquakes, each with a very similar slip, implying that up to half a dozen successive

event ruptures along the Fuyun fault followed a characteristic slip pattern. Although the occurrence of smaller magnitude events, associated with smaller offsets, cannot be completely ruled out, we found no convincing evidence of any.

To test quantitatively how many characteristic slip events each of the 279 displacement values might represent, we model a theoretical distribution of offsets based on the 1931 slip function and the assumption of characteristic coseismic slip. To account for the fact that the number of observations decreases exponentially with increasing offset (Fig. 1), that is, with the number of events and hence with time, we introduce a constant (λ , characterizing the rate of preservation of geomorphic markers) that integrates all degradation factors, natural or anthropological (see Supplementary Method). This constant averages local conditions over the 110 km studied and can be used on a regional basis to quantify the ageing of landforms as a function of time. In a way, it characterizes the resilience of geomorphic memory. Here, along the eastern edge of the Jungar basin, the constant that best fits the dataset in Fig. 1 is $\lambda = 0.55$. Figure 3 shows the results of the modelling in the form of a probability density function (PDF) superimposed on the original dataset, with data points coded by symbols indicating the number of events. The number of events attributed to each measured cumulative offset reflects the highest calculated probability density (see Supplementary Method). The penultimate event is well defined along most of the length of the fault studied, with cumulative offsets twice as large as the smallest offsets associated with the 1931 earthquake. The third event back in time is also well defined between 5 and 75 km. Despite sparser data, the fit between measured offset and predicted event number remains satisfactory for the fourth and fifth events, especially between 47 and 65 km. The larger offset values around 37 m, although fewer than ten in number, hint at the possible record of a sixth earthquake. The simple pattern of clear first multiples observed between 5 and 80 km, however, breaks

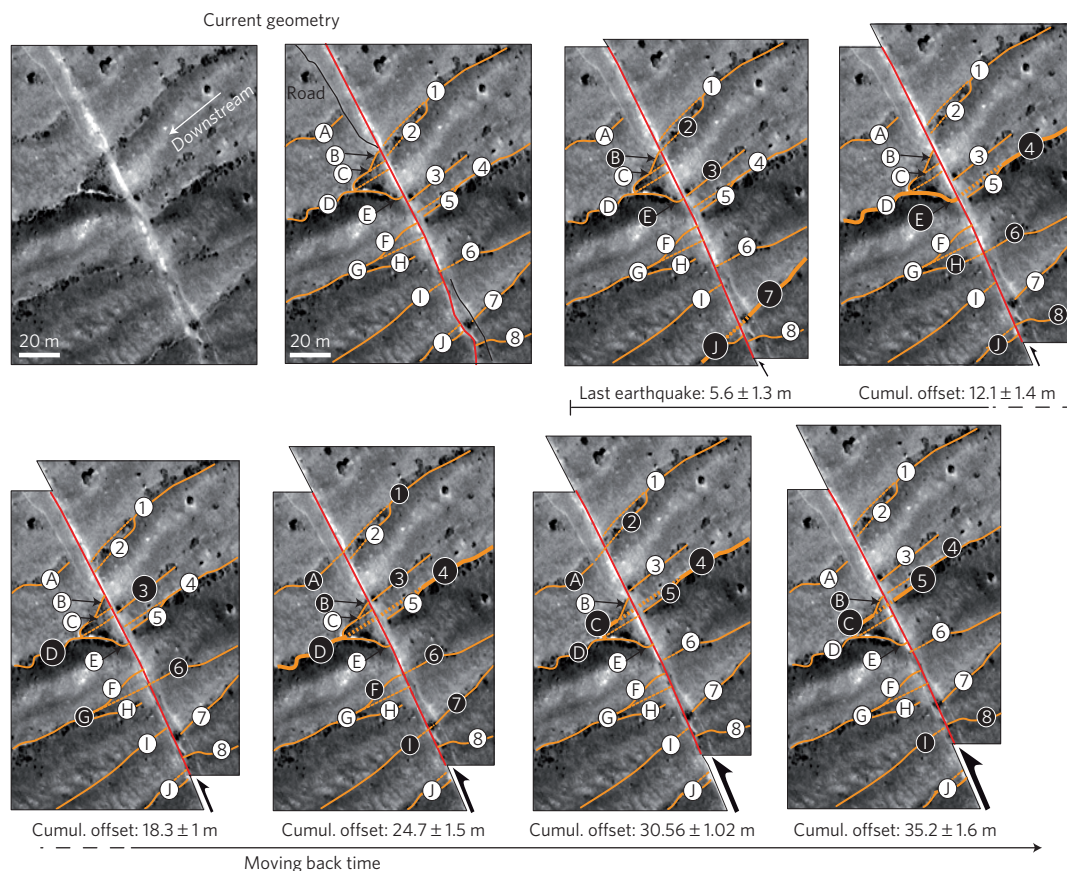


Figure 2 | Successive reconstructions of offset channels at site 4D (location on Fig. 1). Channels are labelled alphabetically and numerically on the west and east sides of fault, respectively. Starting from the present geometry, the east side is moved to realign channels truncated or disconnected as the result of successive earthquakes. Each offset is determined by restoring continuity of one main channel (large black circle) and other secondary channels (small black circles). Successive offsets of 5.6, 12.1, 18.3, 24.7, 30.56 and 35.2 m are identified.

down at the southern end of the rupture. This is also where the two independent field surveys^{17,22} depart most significantly from one another. This may be taken to indicate the existence of additional offsets resulting from an earthquake other than the 1931 event, for which the rupture might have propagated northwards from the southernmost stretch of the fault south of Ertai.

Overall, our ‘Quickbird’ dataset indicates that local coseismic slip for successive earthquakes on the central 80 km of the Fuyun fault was very similar, pointing to a characteristic slip behaviour¹. The successive ruptures seem to have propagated across step-overs as wide as 2.2 km, as observed elsewhere¹⁰. As no direct dating is available for the cumulative offsets, the ages of earthquakes predating 1931 are unknown. Hence, it remains possible that such earthquakes ruptured only part of the stretch of the fault that slipped during the last event. However, the facts that the two main segment boundaries are not strongly expressed geomorphically and that neither is well marked in the 1931 slip distribution make this unlikely. Moreover, any such earthquake would have had an unduly large slip relative to rupture length, an observation clearly at odds with general scaling laws. This does suggest that the last five earthquakes on the fault were close to characteristic, a rather unexpected circumstance along strike-slip faults¹, but not altogether implausible here. Indeed, in this northernmost boundary zone of the India/Asia collision zone, the present deformation is fairly complex and slow. It is absorbed by several rather short fault systems which slip at only a few mm yr⁻¹ (refs 28,30) and have finite offsets of at most a few tens of km (~25 km for the Fuyun fault, Fig. 1). It is thus likely that even strike-slip faults here are in an immature stage of development and still growing. Clearly,

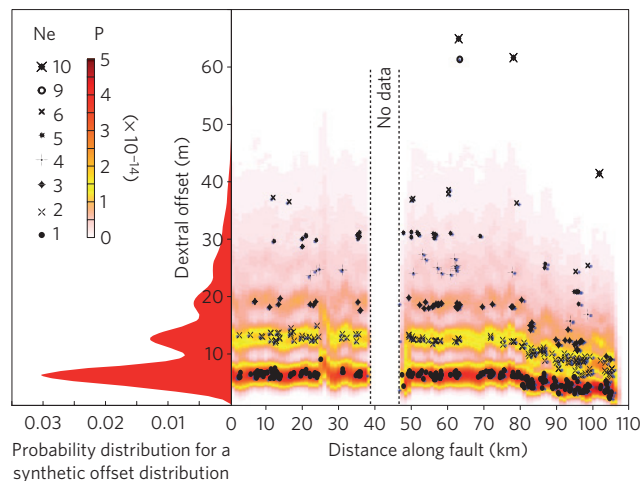


Figure 3 | Direct slip distribution modelling. Comparison between measurements and synthetic density probabilities (P) computed from 1931 initial slip distribution, assuming characteristic slip and exponential decay of landforms. Offset values are coded with symbols representing the most probable number of earthquakes (Ne) required to create them.

dating the occurrence of past earthquakes on the different segments of the fault is the only way to resolve this issue, and determine whether the Fuyun fault still behaves in a characteristic-earthquake mode or if individual segments rupture independently and link opportunistically, producing earthquakes with a more diverse range

of magnitudes and occurrence times, as is usually the case along strike-slip plate boundaries.

Received 25 February 2011; accepted 19 April 2011;
published online 22 May 2011

References

- Sieh, K. The repetition of large-earthquake ruptures. *Proc. Natl Acad. Sci. USA* **93**, 3764–3771 (1996).
- Shimazaki, K. & Nakata, T. Time-predictable recurrence model for large earthquakes. *Geophys. Res. Lett.* **7**, 279–282 (1980).
- Bakun, W. & McEvilly, T. V. Recurrence models and Parkfield, California. *J. Geophys. Res.* **89**, 3051–3058 (1984).
- Weldon, R., Fumal, T. & Biasi, G. P. Wrightwood and the earthquake cycle: What a long recurrence record tells us about how faults work. *GSA Today* **14**, 4–10 (2004).
- Sieh, K. Lateral offsets and revised dates of large earthquakes at Pallett Creek, California. *J. Geophys. Res.* **89**, 7641–7670 (1984).
- Daëron, M. *et al.* 12,000-year-long record of up to 14 paleo-earthquakes on the Yammoûneh fault (Levant fault system). *Bull. Seismol. Soc. Am.* **97**, 749–771 (2007).
- Klinger, Y. *et al.* Paleoseismic evidence of characteristic slip on the western segment of the North Anatolian Fault, Turkey. *Bull. Seismol. Soc. Am.* **93**, 2317–2332 (2003).
- Liu, J., Klinger, Y., Sieh, K. & Rubin, C. Six similar sequential ruptures of the San Andreas fault, Carrizo Plain, California. *Geology* **32**, 649–652 (2004).
- Zielke, O., Arrowsmith, J. R., Grant Ludwig, L. & Akçiz, S. O. Slip in the 1857 and earlier large earthquakes along the Carrizo Plain, San Andreas fault. *Science* **327**, 1119–1122 (2010).
- Wesnousky, S. Predicting the endpoints of earthquake ruptures. *Nature* **444**, 358–360 (2006).
- Klinger, Y. Relation between continental strike-slip earthquake segmentation and thickness of the crust. *J. Geophys. Res.* **115**, B07306 (2010).
- Lindvall, S., Rockwell, T. & Hudnut, K. Evidence for prehistoric earthquakes on the Superstition Hills fault from offset geomorphic features. *Bull. Seismol. Soc. Am.* **79**, 342–361 (1989).
- Kondo, H. *et al.* Slip distribution, fault geometry, and fault segmentation of the 1944 Bolu-Gerede earthquake rupture, North Anatolian Fault, Turkey. *Bull. Seismol. Soc. Am.* **95**, 1234–1249 (2005).
- Tapponnier, P. & Molnar, P. Active faulting and Cenozoic tectonics of the Tien Shan, Mongolia and Baykal regions. *J. Geophys. Res.* **84**, 3425–3459 (1979).
- Ding, G. (ed.) *The Fuyun Earthquake Fault Zone in Xinjiang, China* (Seismol. Press, 1985).
- Kanamori, H. in *Historical Seismograms and Earthquakes of the World* (eds Lee, W. H. K., Meyers, H. & Shimazaki, K.) (Academic, 1988).
- Jianbang, S., Xianyue, S. & Shumo, G. *International Symposium on Continental Seismicity and Earthquake Prediction* (Seismol. Press, 1984).
- Awata, Y., Fu, B. & Zhang, Z. Re-investigation of the geometry and slip distribution of the 1931 Fuyun surface rupture, northwest China. *AGU (Fall meeting Suppl.)* abstr. #no. T41A-1930 (2008).
- Lienkaemper, J. 1857 slip on the San Andreas fault southeast of Cholame, California. *Bull. Seismol. Soc. Am.* **91**, 1659–1672 (2001).
- Rockwell, T. *et al.* Lateral offsets on surveyed cultural features resulting from the 1999 Izmit and Duzce earthquakes, Turkey. *Bull. Seismol. Soc. Am.* **92**, 79–94 (2002).
- Klinger, Y., Michel, R. & King, G. C. P. Evidence for an earthquake barrier model from Mw similar to 7.8 Kokoxili (Tibet) earthquake slip-distribution. *Earth Planet. Sci. Lett.* **242**, 354–364 (2006).
- Lin, A. & Lin, S. Tree damage and surface displacement: The 1931 M 8.0 Fuyun earthquake. *J. Geol.* **106**, 751–757 (1998).
- Wells, D. L. & Coppersmith, K. J. New empirical relationships among magnitude, rupture length, rupture width, rupture area, and surface displacement. *Bull. Seismol. Soc. Am.* **84**, 974–1002 (1994).
- Lee, W. H. K., Kanamori, H., Jennings, P. C. & Kisslinger, C. *International Handbook of Earthquake and Engineering Seismology* (Academic, 2002).
- Sieh, K. *et al.* Near-Field investigations of the Landers earthquake sequence, April to July 1992. *Science* **260**, 171–176 (1993).
- Haeussler, P. J. *et al.* Surface rupture and slip distribution of the Denali and Totschunda faults in the 3 November 2002 M 7.9 earthquake, Alaska. *Bull. Seismol. Soc. Am.* **94**, S23–S52 (2004).
- Wesnousky, S. G. Displacement and geometrical characteristics of earthquake surface ruptures: Issues and implications for seismic-hazard analysis and the process of earthquake rupture. *Bull. Seismol. Soc. Am.* **98**, 1609–1632 (2008).
- Calais, E. *et al.* GPS measurements of crustal deformation in the Baikal–Mongolia area (1994–2002): Implications for current kinematics of Asia. *J. Geophys. Res.* **108**, 2501 (2003).
- Shumo, G., Meixiang, B., Daozun, X. & Zhiyong, X. The recurrence intervals of major earthquakes at the active kottokay-Ertai fault. *Earthq. Res. China* **2**, 67–80 (1986).
- Baljinnyam, I. *et al.* *Ruptures of Major Earthquakes and Active Deformation in Mongolia and its Surroundings, Geological Society of America Memoir 181* (The Geological Society of America, 1993).

Acknowledgements

Thanks are extended to the CNES, which gave us access to imagery in the framework of the Pleiade preparation program. We thank R. Arrowsmith and G. Biasi for constructive reviews. This is IGP contribution 3157, and EOS contribution 20.

Author contributions

M. E. carefully mapped offset markers along the fault. C.N. took care of much of the statistical modelling effort. They, and all other authors, equally participated in the completion of the work.

Additional information

The authors declare no competing financial interests. Supplementary information accompanies this paper on www.nature.com/naturegeoscience. Reprints and permissions information is available online at <http://www.nature.com/reprints>. Correspondence and requests for materials should be addressed to Y.K.